공학석사 학위논문

Rheological properties of poly(butylene adipate-co-terephthalate) / poly(lactic acid) blends and their relation with morphology

폴리부틸렌테레프탈레이트와 폴리락틱산 블렌드의 모폴로지와 유변학적 특성의 연관성 연구

2022 년 8 월

서울대학교 대학원
화학생물공학부

정혜영

폴리부틸렌테레프탈레이트와 폴리락틱산 블렌드의 모폴로지와 유변학적 특성 연관성

지도 교수 안경현

이 논문을 공학석사 학위논문으로 제출함

2022 년 8 월

서울대학교 대학원
화학생물공학부
정혜영

정혜영의 공학석사 학위논문을 인준함
2022 년 8 월

위 원 장 오 준 학 (인)

부위원장 안 경 현 (인)

위 원 김 소 연 (인)

Abstract

Rheological properties of poly(butylene adipate-co-terephthalate) / poly(lactic acid) blends and their relation with morphology

Hye Young Chung
School of Chemical and Biological Engineering
The Graduate School
Seoul National University

In this study, PBAT/ PLA blend is investigated based on rheological, morphological, and mechanical measurements. PLA and PBAT have complementary properties, so there are many researches about their blending. The blending of PBAT with PLA revealed the enhancement of the PBAT' s strength. PBAT 90wt%/ PLA 10wt% blend was prepared through multiple steps of mixing processes in internal mixer in order to modify blend morphology determining blend performances. 1st step is producing PBAT/PLA masterbatches which have different ratio between PBAT and PLA, and 2nd step is dilution of masterbatches with PBAT to adjust same PLA contents in final product. The melt in PBAT at $T_{m,PBAT} < T_{m,processing} < T_{m,PLA}$ to maintain the 1^{st} step PLA morphology in a final product. Through this mixing method, various blend morphologies ranging from droplet to ellipsoids with different aspect ratio could be obtained. According to the rheological measurements, it was

found that the non-spherical PLA domain enhanced the elastic modulus of blends significantly. Moreover, the results showed that shear-thinning tendency of blends became also stronger as the morphology of the dispersed PLA domains become non-spherical. The tensile results show that multi-step mixing samples resulted in improvement of yield strength and modulus.

Our results provide compelling evidence that the rheological and mechanical properties can be changed by morphology control. This study suggests that the inducing of non-spherical morphology in PBAT/PLA blend is a method to overcome drawbacks of PBAT without losing the biodegradability.

Keyword: PBAT, PLA, blend, morphology control, non-spherical, multiple step mixing
Student Number: 2020-25496

Table of Contents

List of Figures

Chapter 1. Introduction

1.1. Study Background

Poly(butylene adipate-co-terephthalate) (PBAT) is a biodegradable polymer that has attracted much attention due to its biodegradation and high ductility. PBAT is 100% biodegradable biopolymer, which is aliphatic aromatic polyester consisting of two types of comonomer, butylene terephthalate segment, and butylene adipate segment. It has been investigated as a potential material for a variety of applications ranging from agricultural films to medical devices [1]. The glass transition temperature of PBAT is about -30℃, which means it is ductile material at room temperature [2]. However, poor heat resistance and inferior stiffness limit its wider industrial applications [3]. Thus, many researches are continued to resolve these limitations.

To overcome above drawbacks of neat PBAT without losing the biodegradability, several studies have been carried out blending with other polymers. A few polymers that can be considered are poly(butylene succinate) (PBS) [4], poly(lactic acid) (PLA) [5,6], poly(hydroxyalkanoate) (PHA) [7], poly(caprolactone) [8].

Among these biodegradable polymers, melt blending with PLA can be the most useful strategy to tailor the performance of the final product from a ductile material(PBAT) to a brittle one(PLA). PLA is polyester based biodegradable polymer, which is derived from corn starch. It possesses superior mechanical properties, such as modulus and strength, so one of the most popular candidate materials to substitute for several petroleum-based polymers [9]. Moreover, PLA has transparent and good barrier properties, so it is known as suitable material for food packaging [10].

There are a few studies regarding flexible PBAT and stiff Polylactic acid(PLA) melt blending. For example, Ke Li et al. tested PBAT/PLA blends using a dynamic rheometer to study

rheological behavior in the wide range of compositions and concluded a phase inversion occur as the PBAT contents reached about 30wt%, leading to decreased of η^*, G', and G"[11]. Shen su et al. reported that the PLA contributes the improvement of the mechanical property, especially modulus of elasticity and tear propagation resistance of blends [12]. Yixin Deng et al calculated the volume fractions at which the dispersed phase morphology of PBAT/PLA blends turned into a co-continuous structure. They used melt viscosity ratio to predict morphology change point, and confirmed that there are other properties changes as well, such as phase morphology, mechanical property, thermal property [13].

So far, most of the studies on PBAT/PLA blends have mainly focused on only the complementary effect by tailoring the blend ratio between two polymers. Only a few studies have explored the influence different morphology of PLA as dispersed phase. PBAT/PLA blends could extend its applications into versatile areas by controlling the morphology of dispersed phase. Researches already widely discussed that the needs for diversify morphology between the phases in order to make synergistic effects of each polymer. The Macosko group investigated microstructure development in immiscible polymer blends, which are produced by melt compounding in extruder [14]. They reported that droplet like blend morphologies could greatly improve the high toughness performance of the matrix, while diffusion barrier performance could be enhanced in lamellar blend structure. Also, co-continuous morphologies could affect electrical conductivity, and these morphologies could be created through stopping melt blending process at different stages. Finer morphology contributes to better formability with larger expansion ratio [15]. This could be likely due to the improved melt strength which hampers the expansion suppression. Finer morphology could be obtained through twin

screw extruder which has more severe shear and elongation deformation than in internal mixer. Also, there's a study about improvement of extensional viscosity with the aspect ratio of the fibrils [16]. The rheological properties of fibril dispersed phase are more prominent under the extensional flow than shear flow. The strain hardening behavior was also observed due to restriction stretching of fibrils.

1.2. Purpose of Research

In that respect, this paper presents PBAT/PLA blend system with different morphologies. One interesting approach to control the morphology of these blends an optimized processing condition to prepare PBAT/PLA melt blends with diversify the phase morphology. Moreover, this study focuses on relationships between rheological properties and particular morphology that can be observed during melt mixing. In the same context, controlling of the dispersed phase aspect ratio, diameter and distribution could extremely affect the final properties of a blend as well as the intrinsic properties. The morphology of polymer blends depends on not only the processing condition, but also the viscosity ratio and the interfacial tensions between the polymers [17]. For example, finer morphology can be obtained when the viscosity ratio between the matrix and dispersed phases is closer to one [18]. And also, interfacial tension between the polymers is low, there's a similar effect [19]. There a few studies about these results. J. sun et al. [20] and Xin. Li et al. [21] observed that the use of a proper contents of chain extender could influence the interfacial interactions between the polymer phases and thereby the morphology of the blend. Also, this could be able to influence the extensional viscosity. Moreover, droplet size could be reduced in

the presence of cellulose nanocrystals and nano clay due to interference of droplet coalescence.[22,23,24] This study also investigated how multi-step mixing methods(i.e. master batch method) affected the droplet morphology and hence the rheological properties and mechanical properties. All the results are compared with those obtained for neat PBAT, and conventionally mixed PBAT/PLA blends. Eventually, the synergistic effects of mechanical and crystallization behavior of neat and blend samples are analyzed.

Chapter 2. Experimental methods

2.1 Materials

PBAT(grade Ecoworld, Melt index < 5g/10min at 190℃/2.16kg) was obtained from JinHui Zhaolong, China. PLA (grade 4032D, Melt index 7g/10min according to ASTM D1238 at 210℃/2.16kg) was purchased from Natureworks (USA). The two components were supplied in the form of pellets.

2.2 Blend preparation

The neat polymers were dried in vacuum oven under 80℃ for at least 12 hours before blending process to avoid hydrolytic degradation. For the first step, PLA masterbatches were prepared. The composition of the masterbatches were PBAT/PLA 75wt%/ 25wt%, PBAT/PLA 50wt%/50wt%, and they were made through melt blending using internal mixer(Rheocomp mixer 600, MKE, Korea) at 100rpm for 7minitues at a temperature of 180℃. After that, they were grinded into flakes about 2mm. For the next step, melt blending of the couple of different masterbatches with neat PBAT pellets was conducted using an internal mixer to dilute PLA. The ratio of PLA was fixed at 10wt% in final blend system. The blends were mixed at 50rpm for 7minutes under 140℃, which is lower temperature than the melting point of PLA, to maintain the PLA morphology of first step blend. Table 1 presents the samples names according to the composition. Properties of samples were compared with neat PBAT and PBAT 90wt%/PLA 10wt% blends produced in general mixing method.

After melt blending process, the samples were molded into disk-shape rheological specimens, rectangular shape for testing elongational viscosity, and dog-bone specimens for mechanical testing using hydraulic press at 140℃. The specification of the test specimen is 1mm of thickness and 25mm diameter for disk mold, 0.5mm of thickness for rectangular mold, and 1mm of thickness for

dog-bone mold. Samples were first heated for 3 minutes, then applied pressure for 7 minutes. Then the samples were cooled to room temperature.

2.3 Morphological characterization

The morphology of the PBAT blends was observed using a field-emission gun scanning electron microscope, SEM (Supra 55VP, CarlZeiss, Germany). In order to observe the cross sections of the samples, all samples were cryogenically fractured across the rheological specimens under liquid nitrogen atmosphere. Before the SEM observation, the fractured surfaces were coated with platinum. Image J program was used to measure the diameter of the dispersed phase. Manually traced diameter was utilized to quantify the morphology of the blend based on average diameter and aspect ratio. The number-average diameter(D_n), volume-average diameter (D_v) of the dispersed phase were calculated by

$$Dn = \frac{\sum_i n_i D_i}{\sum_i n_i}$$

$$Dv = \frac{\sum_i n_i D_i^4}{\sum_i n_i D_i^3}$$

where n_i is the number of domains with diameter D_i counted from SEM images of at least 100 droplets.

2.4 Rheological measurements

Dynamic rheological measurements were conducted at 140℃ using a strain controlled rheometer RMS800 (Rheometrics, USA) with a parallel-plate geometry with a diameter of 25mm. All the

tests are conducted in a gap of 1mm. In order to figure out the linear viscoelastic region, strain sweep tests are preceded prior to frequency sweep tests. All the rheological properties were measured within a linear viscoelastic region range between 1~5%.

Stress-growth experiments were carried out at a shear rate of 0.1, 1, 5 s^{-1} to investigate the blend behavior at 140℃. Also, additional experiment was conducted at 5 s^{-1}, 150℃ to cross check with the previous results.

Uniaxial extensional viscosity is measured using extensional viscosity fixture (Xpansion Instruments, USA), which is an accessory equipment of RMS. Samples are tested at strain rates from 0.07 to 0.1 s^{-1} at 130℃. This is optimized condition obtained through a number of repeated experiments. Sample breakage occurs in the initial stages when strain rates higher than 0.1s^{-1}, and sagging of specimen also occurs at higher temperature.

2.5 Mechanical properties

Tensile properties were measured by an Uniaxial Tensile Machine (LF plus, Lloyd instruments Ltd) at a crosshead speed of 50mm/min in accordance with ASTM D638 type v. The tests were performed at a room temperature. The reported value was based on at least five measurements for each sample.

2.6 Crystallization behavior of neat and blend samples

The melting and crystallization behaviors of neat polymers and blends were explored using differential scanning calorimeter, DSC (Discovery DSC, TA instrument). The samples were exposed to 1st heating/cooling/2nd heating cycles between 0℃ to 200℃. Heating and cooling rate were fixed at 10℃/min. The degree of crystallinity,

Xc, was calculated using the following equation:

$$X_c = \frac{\Delta H_m - \Delta H_{cc}}{W \times \Delta H_{m0}}$$

where $\triangle H_m$, $\triangle H_{cc}$, $\triangle H_m^0$ are respectively heating enthalpy of melting, cold crystallization, and melting for 100% crystalline PBAT (114J/g) and 100% crystalline PLA (93J/g) [25,26]. W is the mass fraction of each polymer in the blend.

No.	Name	Samples(wt%)	Mixing method
1	PBAT	PBAT 100%	-
2	PTPLA10	PBAT 90% / PLA 10%	PBAT/PLA
3	PTPLA10-MB25	PBAT / (PBAT 75 % / PLA25 %)	PBAT/Masterbatch
4	PTPLA10-MB50	PBAT / (PBAT 50 % / PLA50 %)	PBAT/Masterbatch

Table 1. Mixing method to prepare the blend and composition

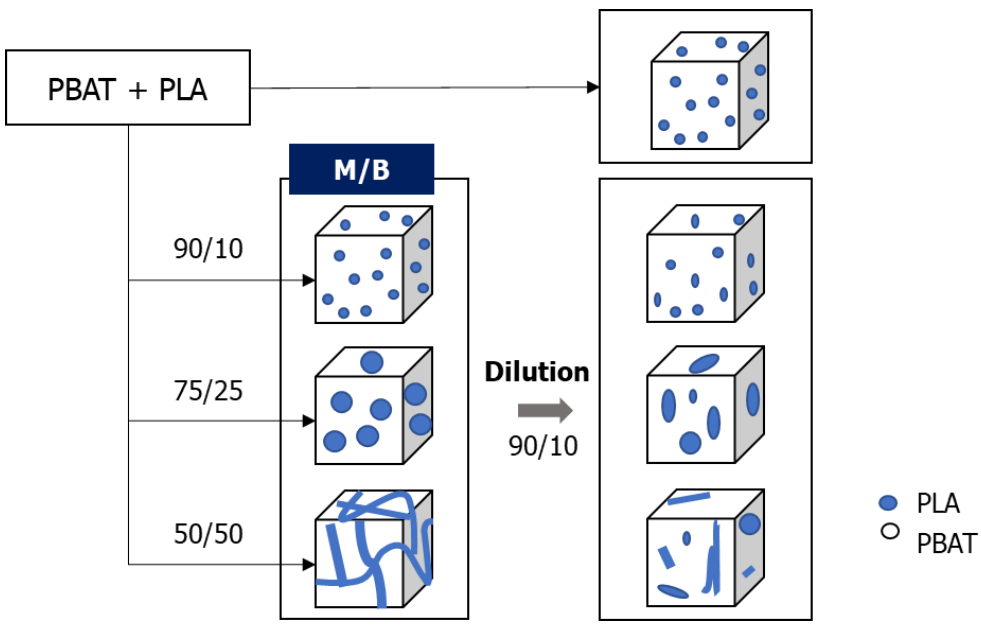

Fig. 1. The proposed mechanism of the morphological change in PBAT/PLA blend system

Chapter 3. Results and discussion

3.1 Morphology of PBAT/PLA blends

The morphology diversification of a polymer blend is accomplished by two steps in the internal mixer. In the first step, the morphologies of the dispersed phase were diversified through masterbatch production that changed the PLA contents. As illustrated in Fig. 2, it is possible to observe the morphology change of dispersed phase as PLA contents increases. Fig. 3 shows the average D_v and D_n of domain increases as the PLA content increases, and the shapes are changed from droplet to co-continuous. In addition, as the content of PLA increases, the tensile strength increases due to PLA with brittle characteristics, however, elongation at break tends to decrease (Fig. 4). These results are consistent with those confirmed by previous studies.[27,28]

In the next step, the masterbatches are diluted with PBAT by melt mixing to make the same PLA contents for all samples as 10wt%. To maintain the morphology of first step, melt blends were processed below the melting temperature of the dispersed PLA phase. At such processing temperature, the dispersed PLA are expected to behave the almost same morphology as first step. Reference systems were also produced under conventional melting conditions, which is a temperature above the melting of both polymers[Fig. 5 (a)]. Fig. 5 (b), (c) depicts the structure of the PLA domain produced by two step mixing method. It can be seen that the shape and size of the dispersion phase in the blend change according to the PLA masterbatch composition. In case of PTPLA10-MB25 sample, the shape of the dispersed phase changes from a spherical to an elliptical shape. The morphology was similar as PTPLA10, which is produced under conventional mixing method, but the aspect ratio is increased from 1.1 to 1.4. The PTPLA10-MB50 has a broad size distribution of dispersed phase. It has a mixture of ellipsoid shaped phase with the mean average diameter

1um and a long plate shaped phase with a length of 20um. And the aspect ratio of PTPLA10-MB50 is also increased to 1.6 as well (Table 2). These morphologies are induced by morphology of first step, and slightly deformed due to uncontrollable shear and other energies during melt mixing. In addition, it can be estimated that the higher the PBAT content in the masterbatch, it melts into the matrix earlier due to the wider the contact area with the diluted PBAT matrix. Thus, as noted earlier, the shape and size of the PLA disperse phase can be varied by multiple step mixing process at a fixed content of 10%, and the aspect ratio can also be controlled.

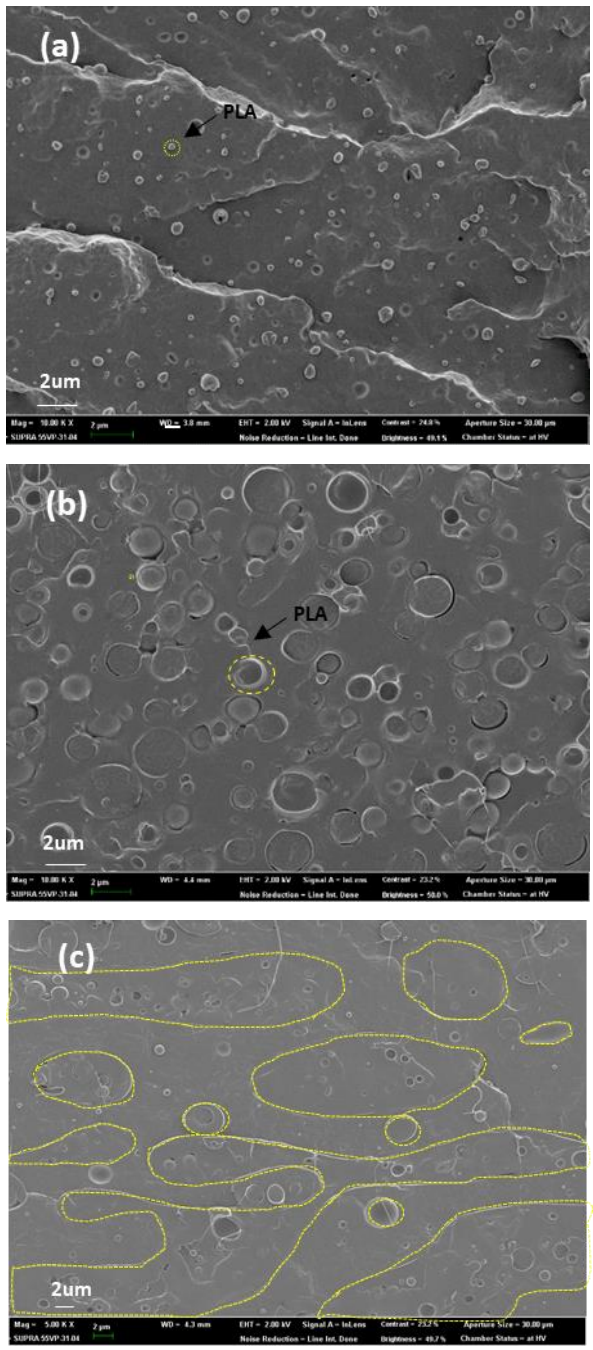

Fig. 2. SEM images of masterbatches which is composed of PBAT/PLA with different weight ratio: (a) 90/10, (b) 75/25. (C) 50/50

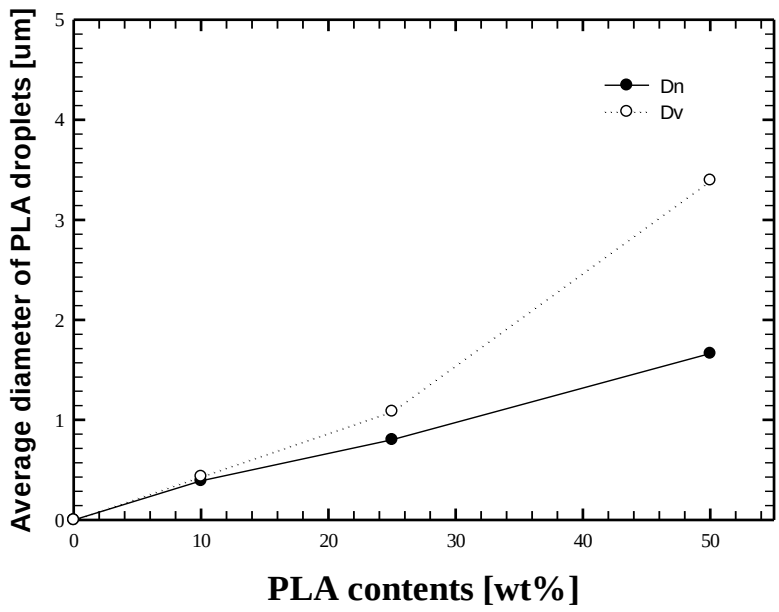

Fig. 3. Number average diameter(D_n)and volume average diameter(D_v) with different PLA contents

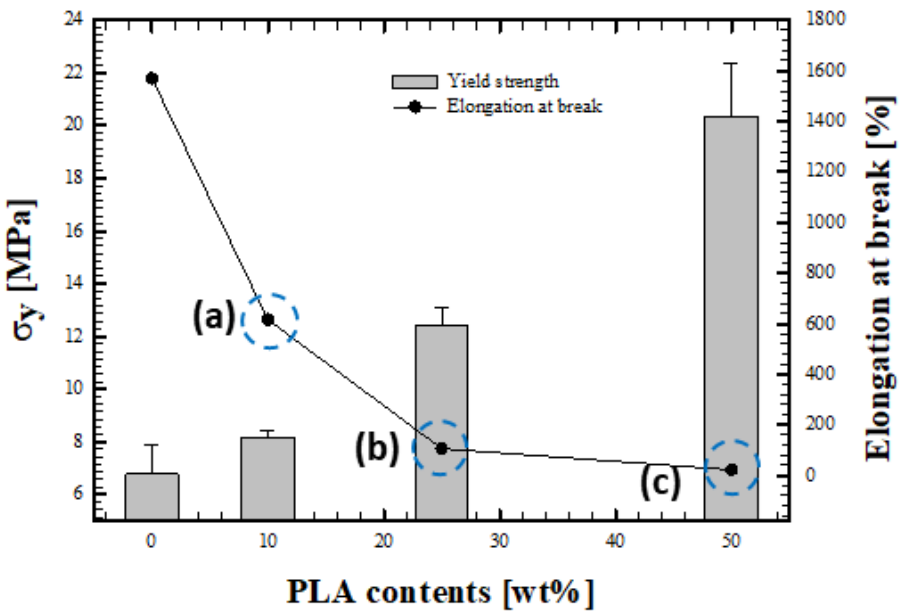

Fig. 4. Yield strength and elongation at break of masterbatches with different PLA contents

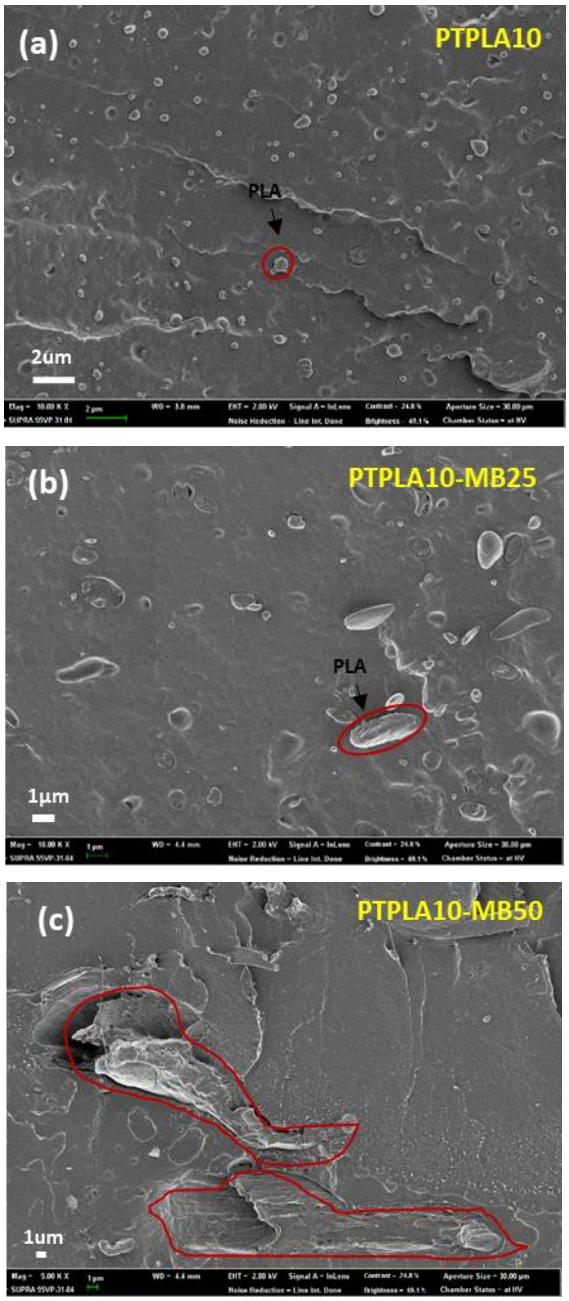

Fig. 5. SEM images of (a) PTPLA10, (b) PTPLA10-MB25, (c) PTPLA10-MB50, showing the different PLA dispersed phase in the PBAT matrix in different blend systems

Sample	Dispersed phase				
	Shape	Aspect ratio	Size [um]		
			Diameter	Width	Length
PTPLA10	Droplet	1.18	0.44	–	–
PTPLA10 -MB25	Ellipsoid	1.40	–	0.61	0.85
PTPLA10 -MB50	Long plate	1.52	–	1.08	1.80
			–	2.75	6.11

Table 2. Shape and dimensions of PLA domains in various PBAT/PLA blends as revealed from SEM images

3.2 Shear response in the linear viscoelastic region

In order to analyze the morphology of the PBAT/PLA blend in detail, storage modulus G' and loss modulus G" are compared depending on the morphology changes. Fig. 6 (a) and (b) show the frequency sweep test results for the neat PBAT and blend systems at 140℃. In the case of neat PBAT, the mixing was performed at 180℃ to equalize the heat history with blend. The low frequency region reflects the long-term behavior of the blends, so the value was compared at 0, 1 rad/s. The storage modulus of neat PBAT is 20Pa, while PLA 10% blends has two times higher value. On the other hand, the storage modulus of the PLA masterbatch blend systems is increased to higher values at low frequencies compared to the conventional blend due to interfacial effects. PTPLA10-MB25 and PTPLA10-MB50 with a non-spherical dispersed phase are 80 Pa, 80Pa respectively, these are higher value than PTPLA10, so the results show that the improvement of elasticity and melting strength as the interfacial tension changes between anisotropic PLA dispersed phase and the matrix.

As shown in Fig 6 (b), the complex viscosity(η^*) of PTPLA10-MB25, PTPLA10-MB50 is higher than that of PTPLA10, and also that of PBAT. In particular, PTPLA10-MB50 exhibits a higher compared to the PTPLA10-MB25, which is due to the large atypicality of the dispersed phase of PTPLA10-MB50. The low frequency upturn shift observed in the complex viscosity of the blends reflects the shape relaxation of the dispersed PLA. [29] PBAT and PTPLA10 show a plateau at low frequency region below 1 rad/s, however, PTPLA10-MB25, PTPLA10-MB50 exhibit shear thinning behavior in the all frequency region. These results suggest that the non-spherical dispersed phase behaves like a solid particle and inhibits the polymer chain behavior of the matrix, thereby increasing the storage modulus and complex viscosity.

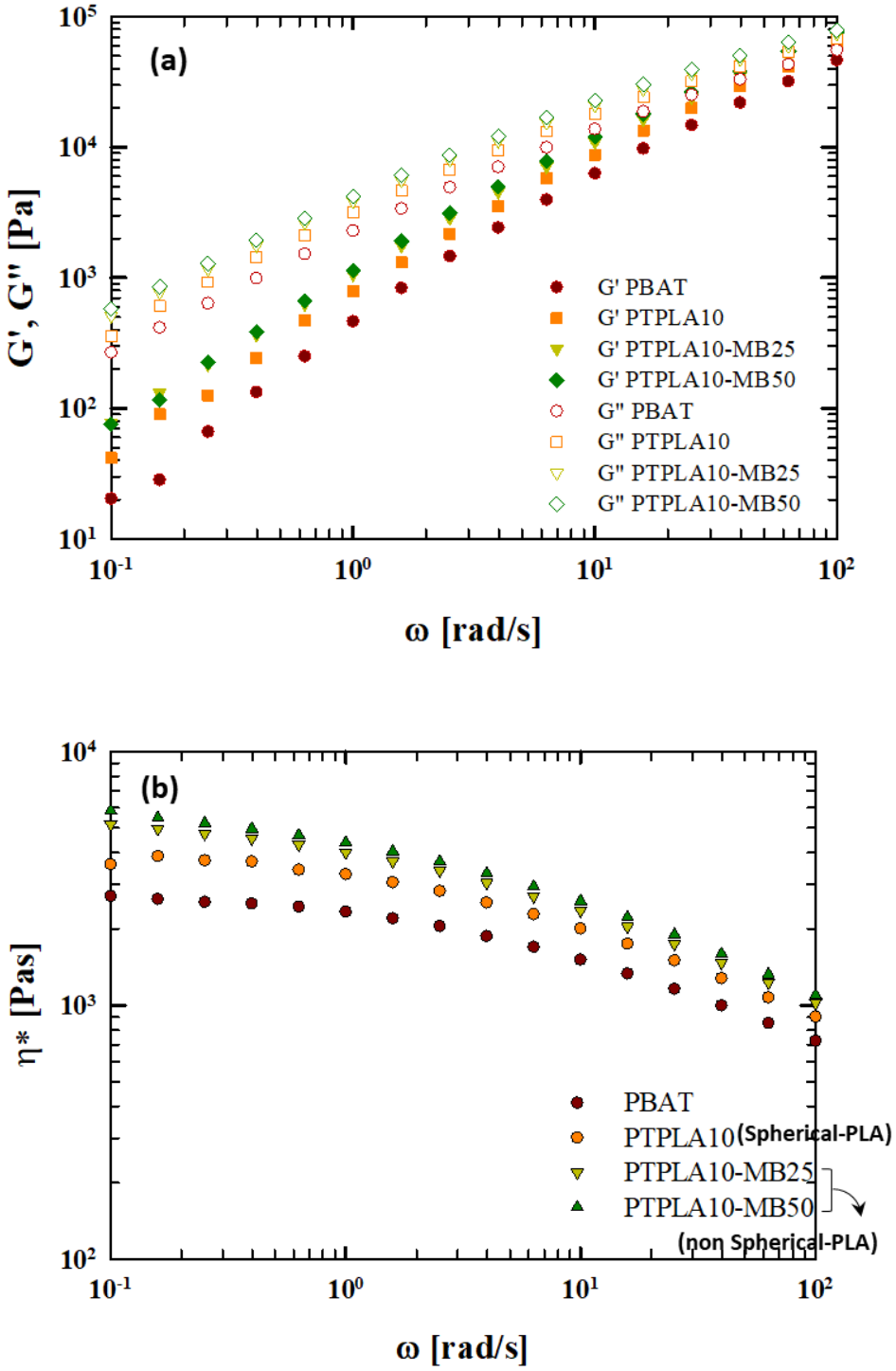

Fig. 6. Storage, loss modulus(a) and complex viscosity(b) of the PBAT/PLA blends as functions of angular frequency at 140℃

3.3 Stress growth behavior

Fig. 5 reports the transient shear viscosity in stress growth experiments of the PLA/PBAT blends at an imposed shear rate of 0.1, 1, 5 s^{-1}. To verify whether the reason for the higher G' value in the low frequency is due to the non-spherical dispersed phase, transient shear rheology test was carried out. The experiment was conducted until the strain reached 50, so that lasted 500s, 50s, and 10s, respectively. The reason why the strain is set to 50 is that the limit time for not flowing out the polymer melts from the plate is 10 seconds at shear rate $5s^{-1}$.

The stress response starts at zero and increased exponentially to the steady state. Previous studies have shown that overshoot at short time is assigned to the network between filler and matrix [24], and decreasing viscosity with time indicates coalescence of droplets [29]. Fig. 7 a~c shows the results of the same experiments for the PBAT/PLA blend, but no appreciable overshoots and viscosity drops were observed at 140℃. However, from a different point of view, the viscosity of PTPLA10-MB25 and PTPLA10-MB50 with a non-spherical PLA dispersed phase shows the higher viscosity than PTPLA10 in the entire time range similar to the tendency of frequency sweep test. These results are same at 0.1, 1, 5 s^{-1}. The max viscosity of PBAT, PTPLA10, PTPLA10-MB25, and PTPLA10-MB25 were, respectively, 2029, 3248, 3509, 3803 Pas at shear rate $5s^{-1}$. This means the PBAT/PLA blends prepared by the masterbatch method had higher viscosity than conventional method in large deformation. In other words, in the blend in which the non-spherical PLA domain is formed, and the domain acts as a filler. Therefore, it can be estimated that the blend shows solid like behavior. Especially PLPLA10-MB50 has higher aspect ratio size of dispersed phases, it reduces the structural deformation of the blend.

In order to reconfirm the previous results, the experiment was conducted at 150℃, $5s^{-1}$ which is large deformation.(Fig. 7d) As a result, the viscosity scale decreased compared to the previous measurement at 140℃, but the deviation between samples was more clearly observed and the tendency was the same. In addition, it was possible to observe the shape of the overshoot of PTPLA10-MB25 and PTPLA10-MB50 in comparison with the neat PBAT within 4 seconds. Also, the viscosity at the steady state shows higher value. Non-spherical domain which is acted like filler inhibits the motion of the polymer matrix chain.

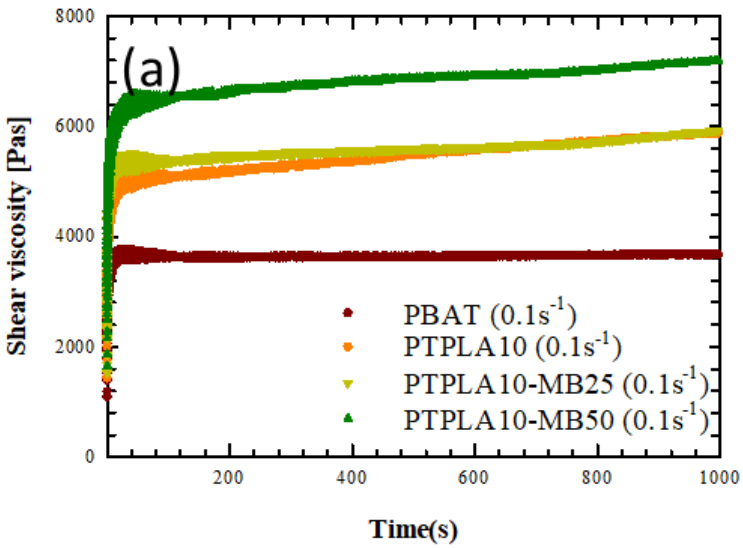
(a)
Shear viscosity [Pas]
Time(s)
PBAT (0.1s-1)
PTPLA10 (0.1s-1)
PTPLA10-MB25 (0.1s-1)
PTPLA10-MB50 (0.1s-1)
0
2000
4000
6000
8000
200
400
600
800
1000

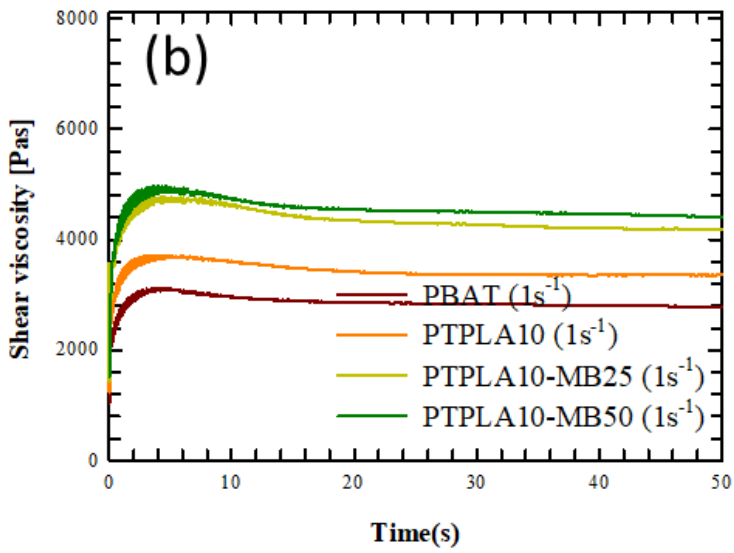
(b)
Shear viscosity [Pas]
Time(s)
PBAT (1s-1)
PTPLA10 (1s-1)
PTPLA10-MB25 (1s-1)
PTPLA10-MB50 (1s-1)
0
2000
4000
6000
8000
0
10
20
30
40
50

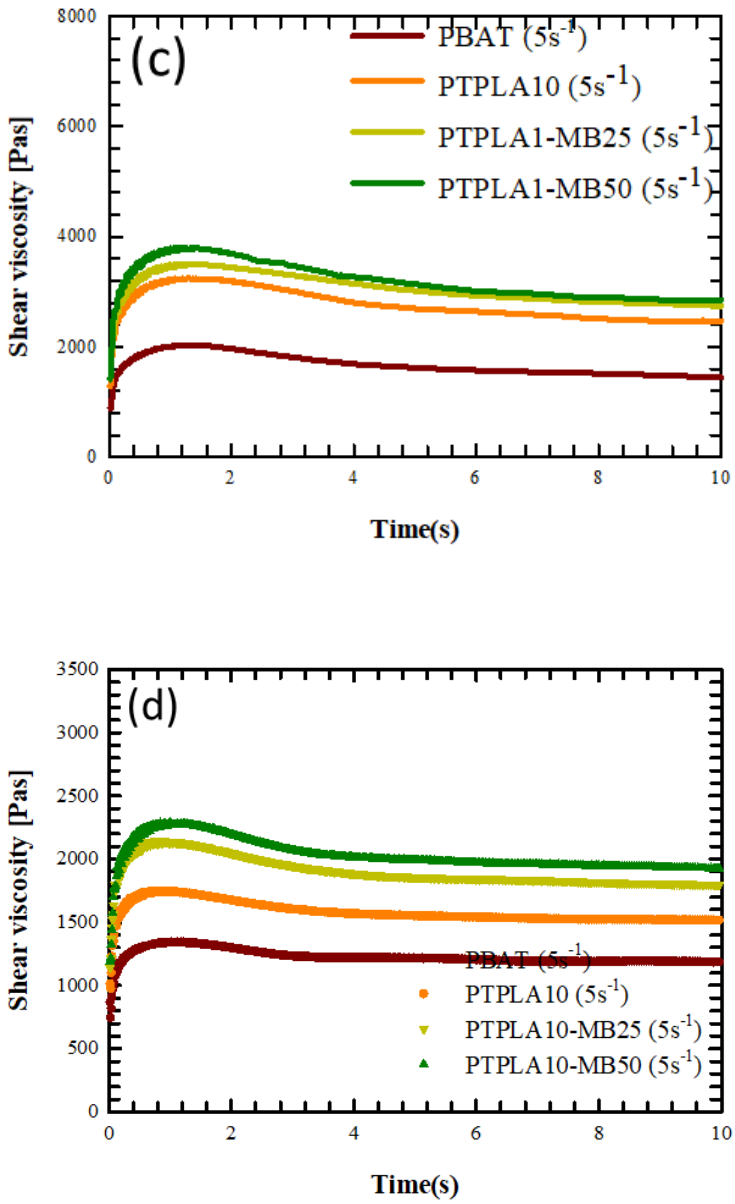

Fig. 7. Transient shear viscosity of PBAT, PTPLA10, PTPLA10-MB25, PTPLA10-MB50 during shearing for various rates at 140℃ (a~c) and 150℃ (d)

3.4. Uniaxial extensional flow response

Fig. 8 illustrates the uniaxial extensional viscosity, η_e^+ , at different extensional strain rates, ε , for PTPLA10(spherical PLA), PTPLA10-MB25(ellipsoid PLA), and PTPLA10-MB50(big plate PLA). The black line in the figures represents the linear viscoelastic prediction of extensional viscosity, $3\eta_e^+$, where is obtained from step rate test at a strain rate of $0.01s^{-1}$. As mentioned above, the experiment was conducted at various temperature conditions and speeds, however, the conditions in which the specimen was cut off within the time when the machine could detect without sagging phenomenon were 130℃ and $0.07/0.1\ s^{-1}$. The experimentally determined extensional viscosity for the neat PBAT and PTPLA10 tends to follow the Trouton relationship, which defines extensional flow is the 3-fold linear viscoelasticity:

$$\eta_e^+ = 3\eta_e^+$$

The elongational viscosity of the PBAT increases until it reaches the predicted three times linear viscosity at strain rate $0.07s^{-1}$. When the strain rate was increased to $0.1s^{-1}$, there is upward deviation from the linear viscoelastic prediction.

The extensional viscosity of all PBAT/PLA blends was higher than that of PBAT. PTPLA10 has longer stretching time than PBAT, so it is possible to estimate that PLA affect the strain hardening property of blends. This phenomenon is more pronounced in blends produced by the masterbatch method. In case of PTPLA10-MB25 and PTPLA10-MB50, the extensional viscosity is obviously increased, so strain hardening phenomenon can be clearly observed. Especially strain hardening occurs in initial stage of stretching when strain rate is $0.1s^{-1}$. The strain-hardening phenomenon occurred earlier and more pronounced with the increase of strain rate for all samples.

From the results shown in Fig.6, it seems that the incorporation of non-spherical PLA domain improved the melt strength of PBAT/PLA blends. It can be estimated that filler like dispersed PLA phase with increased aspect ratio restricted the motion of the matrix polymer chain. PTPLA10-MB50 has ununiformed size distribution of dispersed phase, so the extensional viscosity drops earlier than PTPLA10-MB25. This study shows that the strain hardening effect can be induced through morphology differentiation produced through multiple step mixing method.

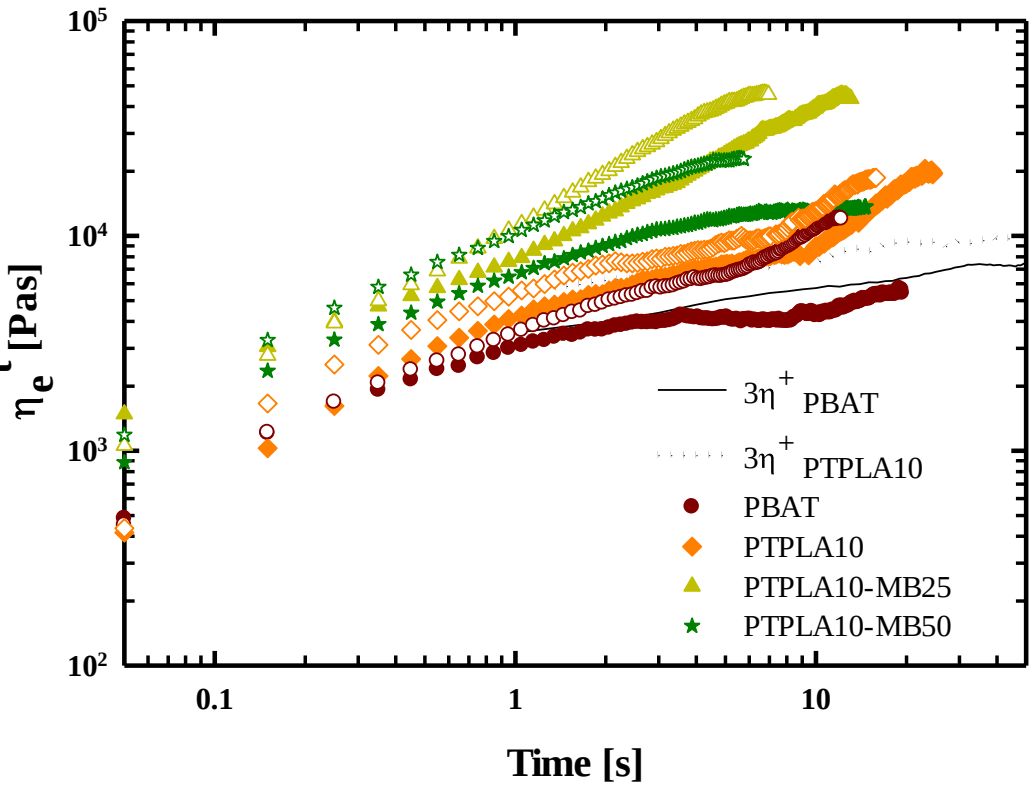

Fig. 8. Uniaxial extensional viscosity of PBAT, PTPLA10, PTPLA10-MB25 and PTPLA10-MB50 measured at temperature of 130℃ and strain rates of 0.07(closed symbol), $0.1s^{-1}$(open symbol). The black lines represent the $3\eta_e^+$, where is obtained from step rate test at a strain rate of $0.01s^{-1}$

3.5. Mechanical property

Stress-strain curves of all the samples and neat PBAT are shown in Fig. 9. As can be seen, the neat PBAT shows high elongation at break over 1500% but low modulus than PLA blends. Similar to the results of previous studies, it was confirmed that the modulus and tensile strength increased when the brittle PLA was blended. Among them, it can be seen that the initial slope of the S-S curve for PTPLA10-MB25 and PTPLA10-MB50 is steeper than that of the conventional blended PTPLA10, more specifically, young's modulus tends to increase. This means that blend samples that induce non-spherical domains affect the mechanical properties of blends.

As shown in Fig. 10, the yield strength of the PBAT/PLA blends are significantly affected by the morphology change. The reason for comparing with yield strength rather than tensile strength is that it is difficult to compare the PLA effect, which accounts for only 10 wt%, due to high elongation property of PBAT. Therefore, the comparison was conducted with the yield strength, which is the strength in the low strain range. Compared to PTPLA10(8.2MPa), the yield strength of PTPLA10-MB25, PTPLA10-MB50 increase to 9.2, 9.3MPa, which increased by around 13%. Considering that the yield strength increased by about 20% from 6.8 MPa to 8.2 MPa by blending PLA with neat PBAT, an improvement in yield strength of 13% is a great effect just by changing morphology at the same PLA content.

Furthermore, the elongation at break of blends was also affected by the morphology change. PTPLA10-MB25 shows the improvement of ductility and toughness of PBAT/PLA blends through increasing aspect ratio of PLA dispersed phase. However, PTPLA10-MB50 shows the decrease of elongation at break because of big domain which makes stress concentrated. The

increasing modulus, yield strength, and elongation at break are probably due to the non-spherical PLA domain. This study shows that an effective method to enhance the mechanical properties of PBAT/PLA blends, the two-steps method was used. The mechanical properties could be improved by using only the different physical properties of couple of polymers, without using any chemical agents.

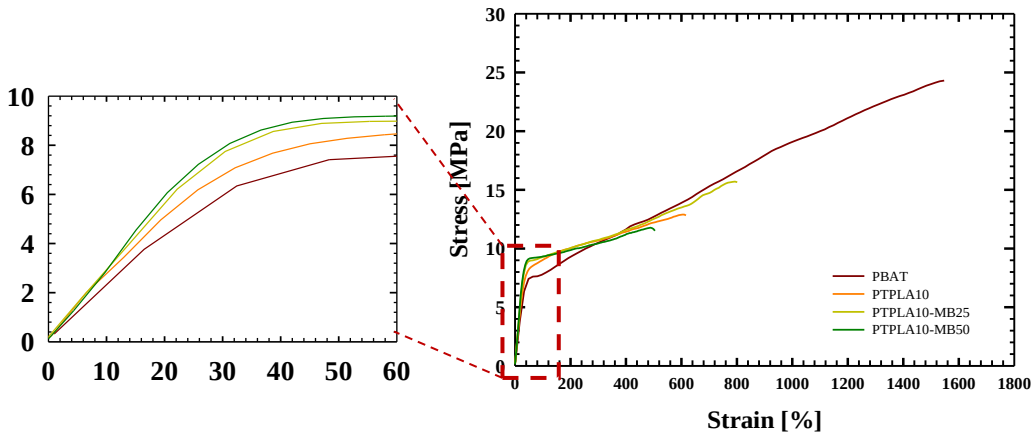

Fig. 9. Tensile strain-stress curves of PBAT, PTPLA10, PTPLA10-MB25, and PTPLA10-MB50 testing at 50mm/min

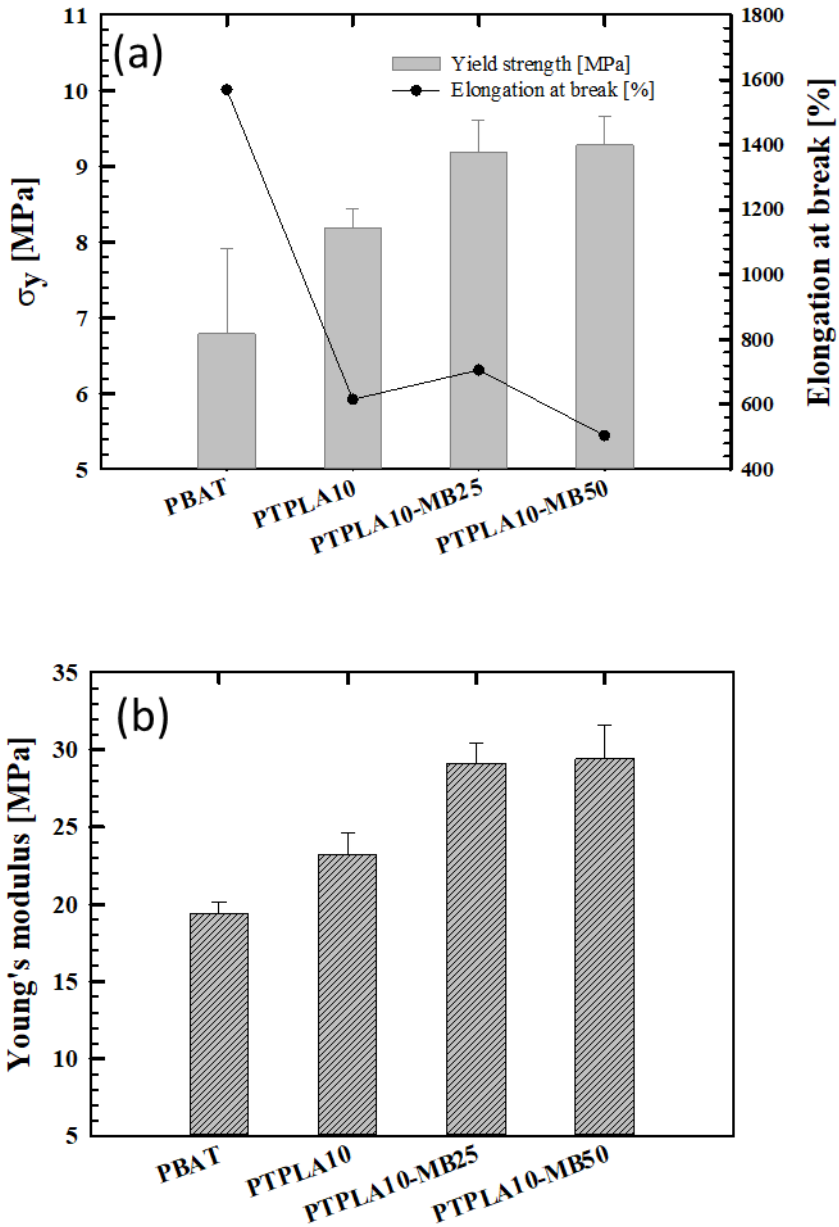

Fig. 10. Yield strength and elongation at break (a), young's modulus(b) of PBAT, PTPLA10, PTPLA10-MB25, and PTPLA10-MB50 testing at 50mm/min

3.6. Crystallization behavior of neat and blend samples

Fig. 11 and Table 3 show the DSC thermograms of PBAT, PLA, and their blends with different mixing methods. In the cooling cycle(Fig. 11a), PBAT showed the one exothermic peak at 78.5℃, whereas PLA showed T_g peak at around 60℃. The PLA incorporation to the PBAT increased the crystalline temperature by 2℃, indicating that the PLA affected crystallization ability of PBAT in the blend. Crystallization peak of PTPLA10-MB25 and PTPLA10-MB50 is shifted towards lower temperature. In other words, the non-spherical induced PLA domain enabled changing of the crystallization ability of PBAT in the blend system.

As for the heating diagram, two times heating were conducted to erase the thermal history. PLA showed the double peak between 150℃ and 155℃. This double peak is commonly showed in polyester based polymers, and related with the melt/re-crystallization/re-melt mechanism [30]. On the other hand, PBAT showed one endothermic peaks at 123℃, which is melting temperature. According to the previous studies, it is known that PBAT showed another additional peak around 60℃, which is attributed to the melting of crystalline phase of BA fraction in PBAT[31]. However, that peak could not be observed in this sample.

In case of blends, there are a few peculiarities were observed. It was observed that the melting peak of PBAT shifted towards high temperature with the blend of PLA. This indicated that PLA restricts the mobility of chains in the blend. However, PTPLA10-MB25 and PTPLA10-MB50 showed lower melting temperature, which is same tendency as in the cooling cycle. Also, around 8% of PBAT Tm crystals are formed in PTPLA10, whereas around 8.6% of PTPLA10-MB25 and 9.0% of PTPLA10-MB50 are generated. The increase in the degree of crystallinity of PBAT can be related

to the morphology changes and this result confirms the rheology and morphology observation results. However, this data needs further verification, because there was an overlap between cold crystal peak of PLA and melting peat of PBAT.

View from a different standpoint, PTPLA10-MB25 and PTPLA10-MB50 reduced degree of PLA crystallinity from 37.4% in the PTPLA10 to 24.6% and 16%, respectively. It can be estimated that the interface area with the PBAT matrix is changed in accordance with morphology change, thus hampering the molecular reorganization and thereby the degree of crystallinity is reduced.

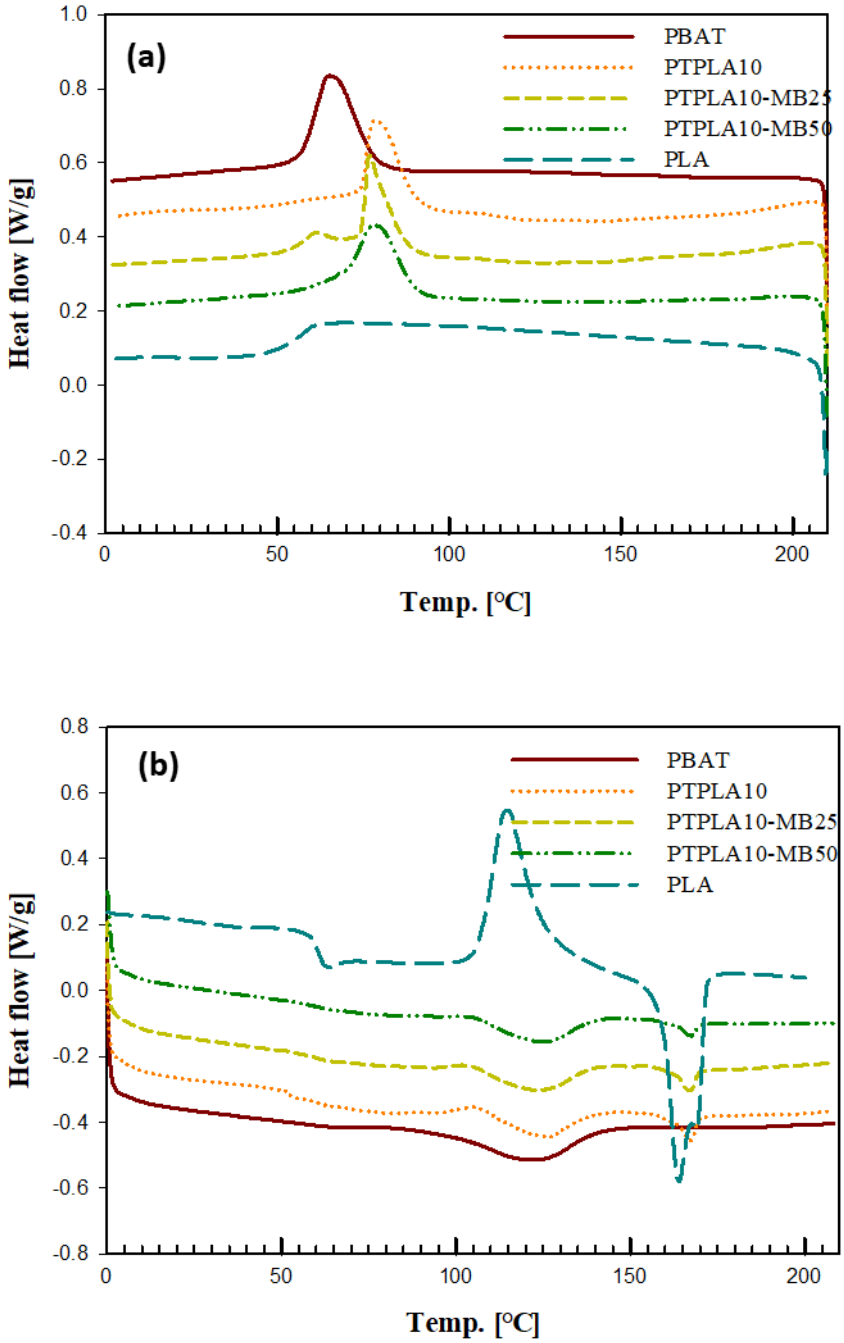

Fig. 11. Cooling(a) and second heating scan(b) of the PBAT, PTPLA10, PTPLA10-MB25, PTPLA10-MB50, and PLA

	T_c (℃)	$\triangle H_c$ (J/g)	T_m^{PBAT} (℃)	$\triangle H_m^{PBAT}$ (J/g)	X_c^{PBAT} (%)	T_m^{PLA} (℃)	$\triangle H_m^{PLA}$ (J/g)	X_c^{PLA} (%)
PBAT	78.5	18.4	123.3	8.0	7.8	-	-	-
PTPLA10	80.6	18.2	126.6	8.0	7.8	167.4	3.5	37.4
PTPLA10-MB25	77.0	18.0	123.8	8.6	8.4	167.1	2.3	24.6
PTPLA10-MB50	78.2	18.7	124.7	9.5	9.3	167.4	1.5	16.0

Table 3. Thermal properties and crystallinity of PBAT, PTPLA10, PTPLA10-MB25, and PTPLA10-MB50

Chapter 4. Conclusion

Prior work has documented the complementary effects of PBAT and PLA polymers; Shen [12], for example, reports that optimized ratio of PBAT/PLA blends contributes the improvement of the PBAT mechanical property especially modulus of elasticity and tensile strength. However, this study just focused on the properties based on blend ratio. In this study we presented the effect of different morphologies to show the relationship with the rheological, mechanical, and thermal properties.

In summary, diverse morphology of PBAT/PLA blends could be obtained under the multistep mixing. We found that blend with non-spherical morphology affect the rheological results exhibited larger melt elasticity and viscosity. Also, elongational viscosity increased in PBAT/PLA blend with non-spherical due to presence of a higher aspect ratio dispersed phase. The tensile tests also showed blend with non-spherical morphology effect on modulus and yield strength. PBAT/PLA blends processed below PLA melting point make solid state PLA which has different morphologies such as ellipsoid and long plate, so these PLA particles which are embedded in PBAT matrix acted as fillers resulting in enhanced property. Our results are in general agreement with previous work, confirming that carrying out the compounding at temperature in a range from below to the melting temperature of the dispersed phase led to high modulus anisotropic composite materials [32]. In addition, this system can reduce the operational costs in industrial process, allowing cost-effective production. This study therefore indicates that the processing condition is one of the crucial factors to make upgraded polymer blends.

Most notably, this is the uncommon study to the knowledge of the authors to provide insight into the tailoring the microstructure affects to rheological property and physical property of polymer blends. Also, it is different from previous studies to induce different

morphologies using the multiple step mixing process and use solid like dispersed phase for fillers. This approach appears to be effective in improving crystallinity of polymer blends, contributing to mechanics. However, optimizing the processing temperature is a complex matter, because there are other variables influence on temperature such as mixer capacity, amount of sample, and etc. Future studies should focus on correlation between processing temperature and other variables to use this polymer blends system for wider applications.

Bibliography

1. Filipe, V.F.; Lucianan, S.C.; Rubia, F.G.; Liliane, M.F. An overview on properties and applications of poly(butylene adipate-co-terephthalate)–PBAT based composites. *Polym. Eng. Sci.* 2020, *3*, 19–26, doi:10.1002/pen.24770.

2. Gigante, V.; Canesi, I.; Cinelli, P.; Coltelli, M. B.; Lazzeri, A. Rubber toughening of polylactic acid (PLA) with Poly (butylene adipate–co–terephthalate)(PBAT): mechanical properties, fracture mechanics and analysis of ductile–to–brittle behavior while varying temperature and test speed. *Eur. Polym. J.* 2019, 115, 125–137, doi:10.1016/j.eurpolymj.2019.03.015.

3. Li, Y.; Zhao, L.; Han, C.; Yu, Y. Biodegradable blends of poly(butylene adipate–co–terephthalate) and stereocomplex polylactide with enhanced rheological, mechanical properties and thermal resistance. *Colloid. Polym. Sci.* 2020, 298, 463–475, doi:10.1007/ s00396–020–04636–1.

4. Zaverl, M.; Valerio, O.; Misra, M.; Mohanty, A. Study of the effect of processing conditions on the co-injection of PBS/PBAT and PTT/PBT blends for parts with increased bio-content. *J. Appl. Polym. Sci*. 2015, 132(2), doi:10.1002/app.41278.

5. Weng, Y. X., Jin, Y. J., Meng, Q. Y., Wang, L., Zhang, M., & Wang, Y. Z. Biodegradation behavior of poly (butylene adipate–co–terephthalate) (PBAT), poly (lactic acid) (PLA), and their blend under soil conditions. *Polym Test.* 2013, 32(5), 918–926, doi:10.1016/j.polymertesting.2013.05.001.

6. Al–Itry, R.; Lamnawar, K.; Maazouz, A. Reactive extrusion of PLA, PBAT with a multi–functional epoxide: Physico–chemical and rheological properties. *Eur. Polym. J.* 2014, 58, 90–102, doi:10.1016/j.eurpolymj.2014.06.013.

7. Tanadchangsaeng, N.; Khanpimai, D.; Kitmongkonpaisan, S.; Chobchuenchom, W.; Koobkokkruad, T.; Sathirapongsasuti, N. Fabrication and characterization of electrospun nanofiber films of PHA/PBAT biopolymer blend containing chilli herbal extracts (capsicum frutescens L.). *J Food Eng.* 2016, 2(1), doi: 10.18178/ijfe.2.1.61-65.

8. Sousa, F. M.; Costa, A. R. M.; Reul, L. T.; Cavalcanti, F. B.; Carvalho, L. H.; Almeida, T. G.; Canedo, E. L. Rheological and thermal characterization of PCL/PBAT blends. *Polym. Bull.* 2019, 76(3), 1573-1593, doi:10.1007/s00289-018-2428-5.

9. Mangaraj, S.; Yadav, A.; Bal, L. M.; Dash, S. K.; Mahanti, N. K. Application of biodegradable polymers in food packaging industry: a comprehensive review. *J Packag Technol Res.* 2019, 3(1), 77-96, doi:10.1007/s41783-018-0049-y.

10. Yadav, A.; Mangaraj, S.; Singh, R.; Kumar, N.; Arora, S. Biopolymers as packaging material in food and allied industry. *Int. J. Chem. Stud.* 2018, 6, 2411–2418.

11. Li, K.; Peng, J.; Turng, L. S.; Huang, H. X. Dynamic rheological behavior and morphology of polylactide/poly (butylenes adipate-co-terephthalate) blends with various composition ratios. *Adv. Polym. Technol.* 2011, 30(2), 150-157, doi:10.1002/adv. 202.

12. Shen, S.; Mona, D.; Rodion, K. Uncompatibilized PBAT/PLA Blends: Manufacturability, Miscibility and Properties. *Materials.* 2020, 13, 4897, doi:10.3390/ma13214897.

13. Deng, Y.; Yu, C.; Wongwiwattana, P.; Thomas, N. L. Optimising ductility of poly (lactic acid)/poly (butylene adipate-co-terephthalate) blends through co-continuous phase morphology. *J. Polym. Environ.* 2018, 26(9), 3802-3816, doi:10.1007/s10924-018-1256-x.

14. Macosko, C. W. Morphology development and control in immiscible polymer blends. *Macromol. Symp.* 2000, 149, 171–184. Weinheim: WILEY-VCH Verlag.

15. Nofar, M.; Tabatabaei, A.; Sojoudiasli, H.; Park, C. B.; Carreau, P. J.; Heuzey, M. C.; Kamal, M. R. Mechanical and bead foaming behavior of PLA–PBAT and PLA–PBSA blends with different morphologies. *Eur. Polym. J.* 2017, 90, 231–244, doi:10.1016/j.eurpolymj.2017.03.031.

16. Hong, J. S.; Ahn, K. H.; Lee, S. J. Strain hardening behavior of polymer blends with fibril morphology. *Rheol. Acta*. 2005, 45(2), 202–208, DOI 10.1007/s00397–005–0015–9.

17. Lee, J. K.; Han, C. D. Evolution of polymer blend morphology during compounding in an internal mixer. *Polymer*, 1999, 40(23), 6277–6296, doi:10.1016/S0032–3861(99)00022–1.

18. Favis, B. D.; Chalifoux, J. P. The effect of viscosity ratio on the morphology of polypropylene/polycarbonate blends during processing. *Polym. Eng. Sci.* 1987, 27(21), 1591–1600, doi: 10.1002/pen.760272105.

19. Favis, B. D. (1991). Polymer alloys and blends: Recent advances. *Can. J. Chem. Eng.* 1991, 69(3), 619–625, doi: 10.1002/cjce.5450690303.

20. Sun, J.; Huang, A.; Luo, S.; Shi, M.; Song, J.; Luo, H. Effect of chain extender on morphologies and properties of PBAT/PLA composites. *J. Thermoplast. Compos. Mater.* 2021, 08927057211051415, doi:10.1177/08927057211051415.

21. Li, X.; Ai, X.; Pan, H.; Yang, J.; Gao, G.; Zhang, H.; Dong, L. The morphological, mechanical, rheological, and thermal properties

of PLA/PBAT blown films with chain extender. *Polym. Adv. Technol.* 2018, 29(6), 1706-1717, doi:10.1002/pat.4274.

22. Nofar, M.; Heuzey, M. C.; Carreau, P. J.; Kamal, M. R. Effects of nanoclay and its localization on the morphology stabilization of PLA/PBAT blends under shear flow. *Polymer*, 2016, 98, 353-364, doi:10.1016/j.polymer.2016.06.044.

23. Sarul, D. S.; Arslan, D.; Vatansever, E.; Kahraman, Y.; Durmus, A.; Salehiyan, R.; Nofar, M. Effect of Mixing Strategy on the Structure-Properties of the PLA/PBAT Blends Incorporated with CNC. *J. Renew. Mater.* 2022, 10(1), 149, doi: 10.32604/jrm.2022.017003.

24. Mohammadi, M.; Heuzey, M. C.; Carreau, P. J.; Taguet, A. Morphological and rheological properties of PLA, PBAT, and PLA/PBAT blend nanocomposites containing CNCs. *Nanomaterials*, 2021, 11(4), 857, doi:10.3390/nano11040857.

25. Herrera, R.; Franco, L.; Rodríguez-Galán, A.; Puiggalí, J. Characterization and degradation behavior of poly (butylene adipate-co-terephthalate) s. *J Polym Sci A Polym Chem* . 2002, 40(23), 4141-4157, doi:10.1002/pola.10501.

26. Fischer, E. W.; Sterzel, H. J.; Wegner, G. K. Z. Z. Investigation of the structure of solution grown crystals of lactide copolymers by means of chemical reactions. *Kolloid-Z. u. Z. Polymere*. 1973, 251(11), 980-990.

27. Jiang, L.; Wolcott, M. P.; Zhang, J. Study of biodegradable polylactide/poly (butylene adipate-co-terephthalate) blends. *Biomacromolecules*, 2006, 7(1), 199-207, doi:10.1021/bm050581q.

28. Pietrosanto, A.; Scarfato, P.; Di Maio, L.; Incarnato, L. Development of Eco-Sustainable PBAT-Based Blown Films and Performance Analysis for Food Packaging Applications. *Materials*, 2020, 13(23), 5395, doi:10.3390/ma13235395.

29. Nofar, M.; Maani, A.; Sojoudi, H.; Heuzey, M. C.; Carreau, P. J. Interfacial and rheological properties of PLA/PBAT and PLA/PBSA blends and their morphological stability under shear flow. *J. Rheol. 2015*, 59(2), 317-333, doi:10.1122/1.4905714.

30. Ma, P. M.; Wang, R. Y.; Wang, S. F.; Zhang, Y.; Zhang, Y. X.; Hristova, D. Effects of fumed silica on the crystallization behavior and thermal properties of poly (hydroxybutyrate-co-hydroxyvalerate). *J. Appl. Polym. Sci.* 2008, 108(3), 1770-1777, doi:10.1002/app.27577.

31. Gan, Z.; Kuwabara, K.; Yamamoto, M.; Abe, H.; Doi, Y. Solid-state structures and thermal properties of aliphatic–aromatic poly (butylene adipate-co-butylene terephthalate) copoly esters. *Polym. Degrad. Stab.* 2004, 83(2), 289-300, doi: 10.1016/S0141-3910(03)00274-X.

32. TZUR, A.; Narkis, M.; Siegmann, A. Immiscible Ethylene Vinyl Acetate and Nylon Blends Processed Below Nylon Melting Temperature. *J. Appl. Polym. Sci.* 2001, 82, 661-671, doi:10.1002/app.1894.